Participation of Two Fusion Peptides in Measles Virus-Induced Membrane Fusion: Emerging Similarity with Other Paramyxoviruses

Orit Samuel and Yechiel Shai*

Department of Biological Chemistry, The Weizmann Institute of Science, Rehovot 76100, Israel

Received July 5, 2000; Revised Manuscript Received October 13, 2000

ABSTRACT: Paramyxoviruses penetrate into their host cells by fusing their membranes with the plasma membrane. The hydrophobic N terminus of their F1 protein, termed the 'fusion peptide', is thought to be responsible for this process. Recently, an additional internal fusion peptide, homologous in sequence to the N-terminal fusion peptide of HIV-1, was identified in the Sendai virus F1 protein. Here, we investigated whether the presence of an additional internal fusion peptide is a general feature of paramyxoviridae. To this end, we synthesized and structurally and functionally characterized three peptides: (i) MV-197, which corresponds to an internal segment of the F1 protein of the measles virus (amino acids 197−225), homologous in location but not in sequence to the internal fusion peptide of the Sendai virus, (ii) Mu-MV-197, a randomized version of MV-197, and (iii) the 33 amino acid N-terminal fusion peptide of the measles virus. Remarkably, only MV-197 was highly fusogenic toward large unilamellar vesicles composed of either zwitterionic (phosphatidylcholine or phosphatidylcholine/sphingomyelin/cholesterol, a composition similar to that of human cell membranes) or negatively charged phospholipids. Binding experiments, circular dichroism spectroscopy in phospholipid membranes, and homo energy-transfer studies with fluorescently labeled peptides revealed that MV-197 adopts a predominant α-helical structure and shares properties similar to those reported for known fusion peptides. These results suggest that the presence of two fusion peptides in the F1 protein is a general feature of paramyxoviruses.

The paramyxoviridae family consists of enveloped negative-stranded RNA viruses, including major human pathogens (*1*). The measles virus, a member of this family, causes a highly contagious disease, which despite the development of a live attenuated vaccine remains a major cause of child mortality in developing countries (*2*). Like other enveloped viruses, measles enters into its host cells by fusion of the viral membrane with the cellular plasma membrane (*3*). Because membrane fusion is an energetically unfavorable reaction, the aid of special viral envelope glycoproteins, called fusion proteins, is required. Despite sharing low sequence homology, most fusion proteins are class I integral membrane proteins, having a short stretch of mostly apolar amino acids, termed the fusion peptide (*4*). To date, two types of fusion peptides have been identified: (i) N-terminal fusion peptides found in most orthomyxoviruses, paramyxoviruses, and some retroviruses (*5*−*9*) and (ii) internal fusion peptides found in the Rous sarcoma virus (*10*), vesicular stomatitis virus (*11*), Ebola virus (*12*), or murine coronavirus (*13*).

Because the process of membrane fusion is complex and involves a wide range of biochemical and biophysical interactions, it is difficult to address the specific role of fusion peptides in the context of the full-length envelope proteins. In attempting to overcome this, researchers have studied the interactions between liposomes or cells and synthetic peptides, corresponding to regions of the intact protein (*14*−*19*). The significance of this approach was demonstrated by the following: (i) the effects of mutations in the whole protein and in the corresponding synthetic peptides are similar (*20*−*28*) and (ii) factors, such as pH or the addition of inhibitory agents, which affect the infectivity of the virus in vivo also affect the activity of the synthetic peptides in vitro (*26*, *29*, *30*).

Paramyxoviridae fusion proteins are synthesized as an inactive precursor, F0, which is activated by a host protease, yielding a transmembrane subunit, F1, and a surface subunit, F2, connected by a disulfide bond (*31*−*33*). The newly formed hydrophobic N terminus of F1 is known as the fusion peptide (*34*, *35*). Although the fusion peptide seems to be directly involved in the process of membrane fusion, it is unlikely that a small N-terminal region of a protein that consists of more than 540 residues controls the entire process. Indeed, it has been shown that additional regions in influenza HA (*36*, *37*) and in HIV-1[1] gp41 (*38*) are able to bind to membranes, suggesting a role for additional membrane-binding regions in the fusion process. In particular, in the Sendai virus F1 protein, the N-terminal and C-terminal heptad repeats and the region following the N-terminal

* To whom correspondence should be addressed. The Harold S. and Harriet B. Bardy Professorial Chair in Cancer Research. Tel: 972-8-9342711. Fax: 972-8-9344112. E-mail: Yechiel.Shai@weizmann.ac.il.

[1] Abbreviations: BOC, butyloxycarbonyl; FMOC, 9-fluorenylmethoxycarbonyl; CD, circular dichroism; DMSO, dimethyl sulfoxide; HF, hydrogen fluoride; HIV, human immunodeficiency virus; LUV, large unilamellar vesicles; NBD-F, 4-fluoro-7-nitrobenz-2-oxa-1,3-diazole; PAM, phenylacetamidomethyl; PBS, phosphate buffered saline; PC, egg phosphatidylcholine; PE, phosphatidylethanolamine; PG, phosphatidylglycerol; SM, sphingomyelin; Chol, cholesterol; RP-HPLC, reverse phase high-performance liquid chromatography; Rho, tetramethylrhodamine; SIV, simian immunodeficiency virus; SUV, small unilamellar vesicles;

10.1021/bi001533n CCC: $20.00
Published on Web 01/11/2001

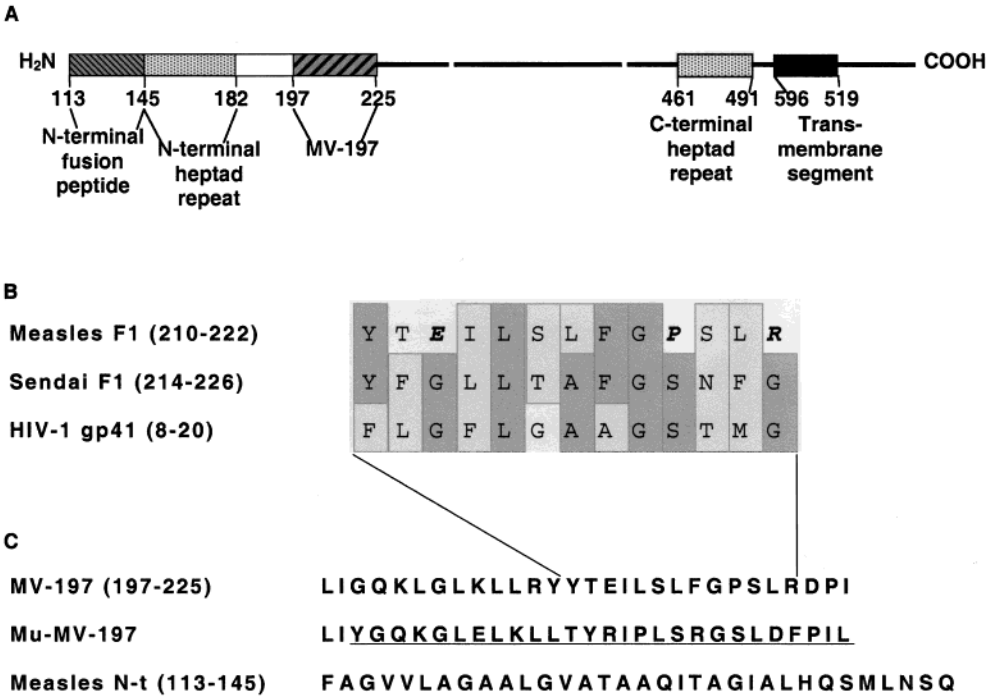

FIGURE 1: (A) Representation of the F1 subunit of the fusion protein of the measles virus. (B) Sequence alignment of the homologous regions between the Sendai F1 protein (amino acids 214−226), HIV-1 gp41 (amino acids 8−20), and the homologous region from the measles F1 protein (amino acids 210−222). A peptide containing amino acids 201−229 from the Sendai F1 protein, analyzed by Peisajovich et al. (*41*), is mentioned in the present study as SV-201. (C) Sequences of the peptides used in the studies. The scrambled sequence of Mu-MV-197 is underlined.

heptad repeat (SV-201) was shown to bind membranes (*39*, *40*). Although the two heptad repeats in the Sendai virus F1 protein do not induce membrane fusion by themselves (*41*), the N-terminal heptad repeat was shown to assist the N-terminal fusion peptide in the fusion process (*28*). Moreover, recently it was found that the region following the N-terminal heptad repeat of the Sendai F1 protein (SV-201), which is homologous in sequence to the N-terminal fusion peptide of HIV-1, induces membrane fusion of large unilamellar vesicles to a larger extent than the Sendai virus N-terminal fusion peptide (*41*). Thus, the N-terminal domain of the F1 protein, including the N-terminal fusion peptide, the heptad repeat, and the adjacent internal fusion peptide, seems to be located close to the membrane and to be involved in the fusion process (Figure 1A). To determine whether a similar N-terminal domain might be a general feature of paramyxoviridae F1 proteins, we decided to test a homologous region to SV-201 in the F1 protein of the measles virus for its ability to induce membrane fusion. Among viruses of the paramyxoviridae family, we chose the measles virus because its putative internal fusogenic region has low homology with the corresponding region in the Sendai virus (*35*). Thus, fusogenic activity of this region would suggest that this feature is general to the paramyxoviridae family. We synthesized the peptide (MV-197) corresponding to amino acids 197−225 of the F1 protein of the measles virus (Figure 1C) and characterized it structurally and functionally. We further synthesized Mu-MV-197, a randomized version of MV-197 and the N-terminal fusion peptide of the measles virus (Figure 1C). MV-197 is homologous in location to the internal fusion peptide found in the Sendai virus. However, instead of two glycines, present both in the internal fusion peptide of the Sendai virus and in the N-terminal fusion peptide of HIV-1, MV-197 contains charged amino acids. In addition, MV-197 contains two prolines, not present in Sendai or HIV-1 fusion peptides (Figure 1B). These major sequence differences were predicted to disturb the fusogenic activity of MV-197. Our findings suggest that the existence of two fusion peptides in the F1 protein is a common feature to the paramyxoviridae family, generalizing the recently revised model proposed for paramyxovirus-induced membrane fusion (*41*).

EXPERIMENTAL PROCEDURES

Materials. BOC-amino acids were purchased from Novabiochem AG (Läufelfingen, Switzerland). BOC-amino acid phenylacetamidomethyl (PAM) resin was obtained from Applied Biosystems (Foster City, CA). *N*-[7-Nitrobenz-2-oxa-1,3-diazole-fluoride] (NBD-F) and other reagents for peptide synthesis were obtained from Sigma. Egg phosphatidylcholine (PC), sphingomyelin (SM), phosphatidylglycerol (PG), and cholesterol (Chol) were purchased from Sigma. *N*-[Lissamine-rhodamine B-sulfonyl]dioleoylphosphatidylethanolamine (Rho-PE), *N*-[7-nitrobenz-2-oxa-1,3-diazole-4-yl]-dioleoylphosphatidylethanolamine (NBD-PE), NBD-F, and 5(and 6)-carboxytetramethylrhodamine (Rho) succinimidyl ester were purchased from Molecular Probes (Eugene, OR). All other reagents were of analytical grade. Buffers were prepared using double-glass-distilled water. Phosphate buffer saline (PBS) is composed of NaCl (8 g/L), KCl (0.2 g/L), KH_2PO_4 (0.2 g/L), and Na_2HPO_4 (1.09 g/L), with pH 7.3.

Peptide Synthesis and Fluorescent Labeling. The peptides were synthesized by a standard solid-phase method on PAM resin (*42*, *43*). NBD and Rho labeling of the N terminus of the resin-bound peptides was achieved, as is previously described (*44*). The peptides were cleaved from the resin by HF treatment and purified by RP-HPLC. The purity (∼99%)

was confirmed by analytical HPLC. The peptide compositions were determined by amino acid analysis.

Preparation of Lipid Vesicles. Small unilamellar vesicles (SUV) were prepared by sonication of PC/PG (1:1) or PC, as is described earlier (*45*). Large unilamellar vesicles (LUV) were also prepared from PC/PG (1:1), PC, or PC/SM/Chol (9:9:2) and when necessary with different amounts of Rho-PE and NBD-PE as follows: Dry lipids were suspended in PBS buffer by vortexing to produce large multilamellar vesicles. The lipid suspension was freeze−thawed 6 times and then extruded 40 times through polycarbonate membranes with 0.1 μm diameter pores (Nuclepore Corp., Pleasanton, CA).

Peptide-Induced Lipid Mixing. Lipid mixing of large unilamellar vesicles was measured using a fluorescence-probe dilution assay (*46*). Lipid vesicles containing 0.6 mol % each of NBD-PE (energy donor) and Rho-PE (energy acceptor) were prepared in PBS, as is described before. A 1:4 mixture of labeled and unlabeled vesicles (110 μM total phospholipid concentration) was suspended in 400 μL of PBS, and a small volume of peptide in DMSO was added. The increase in NBD fluorescence at 530 nm was monitored, with the excitation set at 467 nm. The fluorescence intensity before the addition of the peptide was referred to as 0% lipid mixing, and the fluorescence intensity upon the addition of reduced Triton X-100 (0.05% (v/v)) was referred to as 100% lipid mixing. Reduced Triton X-100 (*47*) was used, as previously done, to prevent quenching of the NBD fluorescence (*26*). All of the fluorescence measurements in the present study were done on a SLM-AMINCO Bowman series 2 luminescence spectrometer.

Electron Microscopy. The effects of the peptides on liposomal suspensions were examined by negative-staining electron microscopy. A drop containing 5.9 mM PC LUV or a mixture of LUV and a peptide at a peptide/lipid molar ratio of 0.037 was deposited onto a carbon-coated grid and negatively stained with phosphotungstic acid (2%, pH 6.8). The grids were examined using a JEOL JEM 100B electron microscope (Japan Electron Optics Laboratory Co., Tokyo, Japan).

Membrane-Binding Experiments. The degree of peptide association with PC/PG (1:1) or PC SUV was determined using NBD-labeled peptides. The sensitivity of the NBD moiety to the dielectric constant of its surroundings allows for the determination of the environment of the NBD-labeled peptides. It has been shown previously that the fluorescence emission of NBD increases and shifts to lower wavelengths upon relocation of the NBD moiety to a more hydrophobic environment (*48*). The changes in fluorescence intensity were measured when adding increasing amounts of SUV to 0.1 μM NBD-labeled peptides dissolved in PBS. Vesicles were added until the increase in the fluorescence was linear because of light scattering caused by the added vesicles alone. The fluorescence intensity was measured as a function of the lipid/peptide molar ratio, with the excitation set at 467 nm (8 nm slit) and the emission set at 530 nm (8 nm slit). The fluorescence values were corrected by subtracting the corresponding blank (PBS with the same amount of vesicles). The maximal fluorescence intensity F_∞ (the fluorescence signal obtained when all of the peptide is bound to lipid) was extrapolated from a double reciprocal plot of F (total peptide fluorescence) vs C_L (total concentration of lipids; *49*). With the knowledge of the fluorescence intensity of the unbound peptide F_0 as well as the bound peptide, F, the fraction of the membrane-bound peptide f_b could be calculated using the formula

$$f_b = (F - F_0)/(F_\infty - F_0)$$

NBD Fluorescence Measurements. Changes in the fluorescence of NBD-labeled peptides were measured upon their binding to vesicles. NBD-labeled peptide (0.1 μM) was added to 2 mL of PBS, containing PC/PG (1:1) or PC SUV (200 μM). The emission spectra were recorded (8 nm slit), with the excitation set at 467 nm (8 nm slit), and compared with the emission spectra of the NBD-labeled peptide in a liposome-free PBS buffer. The lipid/peptide molar ratio was kept at a level such that the majority of the peptides were bound to the vesicles and the contribution of the free peptide to fluorescence could be neglected.

Enzymatic Digestion of Membrane-Bound Peptides. The susceptibility of the peptides to proteolytic degradation in their membrane-bound state was determined as previously described (*50*). Briefly, PC/PG (1:1) or PC SUV (200 μM) added to 0.1 μM NBD-labeled peptide, followed by the addition of 20 μL of Proteinase K (10 mg/mL). The fluorescence intensity at 530 nm (8 nm slit) was recorded as a function of time before and after the addition of the enzyme, and the excitation was set at 467 nm (8 nm slit). In a control experiment, the enzyme was added before the addition of the vesicles.

Rho Fluorescence Measurements. The tendency of the peptides to self-associate in solution and in membranes was tested using Rho-labeled peptides. Because Rhodamine fluorescence intensity is highly sensitive to self-quenching but is only slightly affected by the dielectric constant of its surroundings, changes in the fluorescence intensity of the Rho-labeled peptide may be attributed mainly to changes in its oligomeric state. If the Rho-labeled peptide forms homooligomers, its fluorescence is quenched. When Proteinase K is added, the peptides are cleaved into small peptidic fragments. As a consequence, oligomers, if there are any, dissociate, causing an increase in the fluorescence intensity. Thus, the final Rhodamine fluorescence intensity can be considered as that of a monomeric Rho-labeled peptide. Briefly, Proteinase K (10 mg/mL) was added to 1 μM Rho-labeled peptide either in PBS solution or in the presence of PC/PG (1:1) or PC SUV (3.2 or 8 mM). The fluorescence intensity at 578 nm (8 nm slit) was recorded as a function of time before and after the addition of the enzyme, and the excitation was set at 530 nm (8 nm slit).

Circular Dichroism (CD) Spectroscopy. CD spectra were obtained using an Aviv 202 spectropolarimeter. The spectra were scanned with a thermostated quartz optical cell with a path length of 1 mm, at 25 °C. Each spectrum was recorded with an averaging time of 10 s, at a wavelength range of 260−195 nm. Fractional helicities (*51*) were calculated as follows:

$$f_h = \frac{[\theta]_{222} - [\theta]^0_{222}}{[\theta]^{100}_{222} - [\theta]^0_{222}}$$

where $[\theta]_{222}$ is the experimentally observed mean residue elipticity at 222 nm and values for $[\theta]^0_{222}$ and $[\theta]^{100}_{222}$,

corresponding to 0% and 100% helix content at 222 nm, were estimated at −2000 and −32 000 deg cm^2/dmol, respectively. Each experiment was repeated twice and found to be in good agreement.

RESULTS

Induced Lipid Mixing of LUV by Internal Fusion Peptides and N-Terminal Fusion Peptides. To determine the fusogenic activity of the peptides, we evaluated their ability to induce lipid mixing of LUV by using the fluorescent-probe dilution assay (*46*). Briefly, LUV, labeled with both NBD-PE and Rho-PE, were mixed with unlabeled LUV, and different concentrations of peptides were added. Fusion of labeled and unlabeled LUV, caused by the added peptide, resulted in a dilution of the labeled lipids and a reduction in the energy transfer between NBD-PE and Rho-PE. This change was visualized as an increase in NBD fluorescence. The dependence of the extent of lipid mixing on the peptide concentration was examined. In separate experiments, various amounts of MV-197, Mu-MV-197, and the N-terminal fusion peptide (Figure 1C) were added to a fixed amount of LUV composed of PC, PC/PG (1:1), or PC/SM/Chol (9:9:2). To compare the fusogenic activities of the different peptides, we plotted the percentage of lipid mixing of PC and PC/SM/Chol LUV (Figure 2) as a function of the peptide/lipid molar ratio. Similar results were obtained for PC/PG LUV, and therefore the data are not shown. Our results show that, in contrast to the N-terminal fusion peptide, MV-197 was very active in inducing lipid mixing of LUV. Furthermore, the scrambled peptide Mu-MV-197 showed virtually no activity, suggesting that the fusogenic activity of the peptide depends on its specific sequence. The kinetics of lipid mixing at peptide/lipid molar ratios of 0.08 are shown in the insets of Figure 2. Maximal activities were obtained after 3−4 min.

Peptide-Induced Lipid Mixing and Membrane Fusion. To confirm that the peptide-induced lipid mixing observed was indeed the result of membrane fusion, suspensions of LUV were visualized under an electron microscope before and after the addition of peptides. Briefly, PC LUV, suspended in PBS, were incubated for 10 min either alone, with MV-197, or with Mu-MV-197 before visualization. Representative micrographs of LUV alone, LUV with MV-197, and LUV with Mu-MV-197 are shown in Figure 3, panels A−C, respectively. Panels D−F correspond to A−C, respectively, with 5 times lower magnification. Clearly, MV-197, which was shown to induce lipid mixing (Figure 2), caused an increase in the size of the vesicles. On the other hand, no size increase was observed with Mu-MV-197, which was also inactive in inducing lipid mixing (Figure 2). These results confirm that the ability of MV-197 to induce lipid mixing is the result of membrane fusion.

Membrane-Binding Abilities of MV-197 and Mu-MV-197. The difference between the fusogenic activities of MV-197 and Mu-MV-197 may stem from a difference in their membrane-binding abilities. To test this, we recorded the increase in the fluorescence intensity of the NBD-labeled peptides as a function of the lipid/peptide molar ratio. The sensitivity of the NBD moiety to the dielectric constant of its surroundings allows for the determination of the environment of the NBD-labeled peptides. It has been shown previously that the fluorescence emission of NBD increases

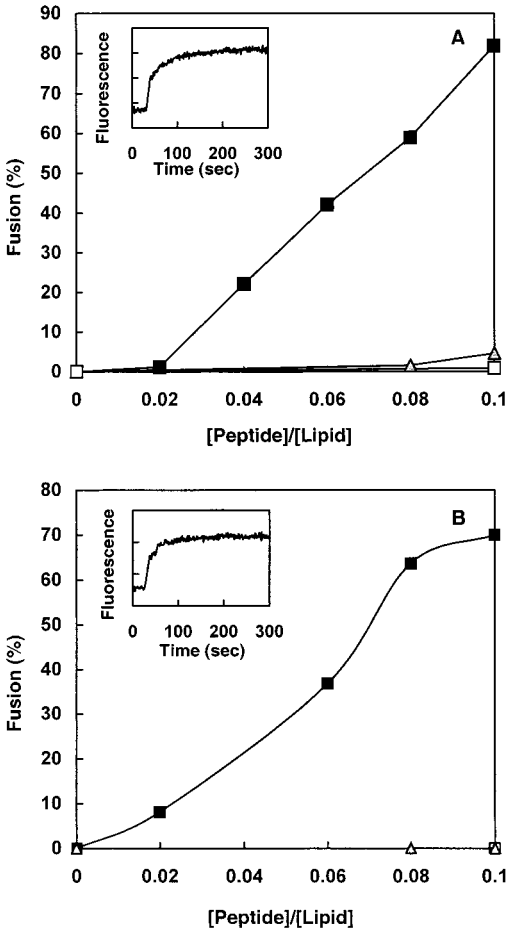

FIGURE 2: MV-197 induces lipid mixing of LUV to a greater extent than the N-terminal fusion peptide of the measles virus. Peptide aliquots were added to mixtures of PC (A) or PC/SM/Chol (9:9:2; B) LUV. The mixture, suspended in PBS, was composed of unlabeled LUV (88 μM) and labeled LUV (22 μM) containing 0.6% each of NBD-PE and Rho-PE. The increase in the fluorescence intensity of NBD-PE was measured 7 min after the addition of each peptide. The fluorescence intensity upon addition of reduced Triton-X-100 (0.05% v/v) was defined as 100%. Symbols: (■) MV-197, (▲) Mu-MV-197, (□) N-terminal fusion peptide. Insets: time course of lipid mixing induced by MV-197, under the same conditions described above, at a 0.08 peptide/lipid molar ratio.

and shifts to lower wavelengths upon relocation of the NBD moiety to a more hydrophobic environment (*48*). The binding curves obtained with PC and PC/PG (1:1) SUV are shown in Figure 4, panels A and B, respectively. These binding curves can be used to evaluate the partition coefficient of binding (*52*). However, because MV-197 self-associates in solution (as shown in Figure 6), the binding isotherms were not further analyzed. The binding curves of MV-197 reached saturation at a lipid/peptide molar ratio similar to that obtained for other NBD-labeled membrane-binding peptides (*53*), suggesting a partition coefficient on the order of 10^4−10^5 M^{-1} for MV-197 in both types of membranes. In contrast, the binding curve of Mu-MV-197 reached saturation at a higher lipid/peptide molar ratio, suggesting a lower partition coefficient for Mu-MV-197 in PC/PG vesicles. Furthermore, although the binding curves of MV-197 to PC and those of MV-197 to PC/PG SUV were similar, the binding of Mu-MV-197 to PC SUV was not detected. As shown, Mu-MV-197 does not seem to bind PC SUV and only about 10% of

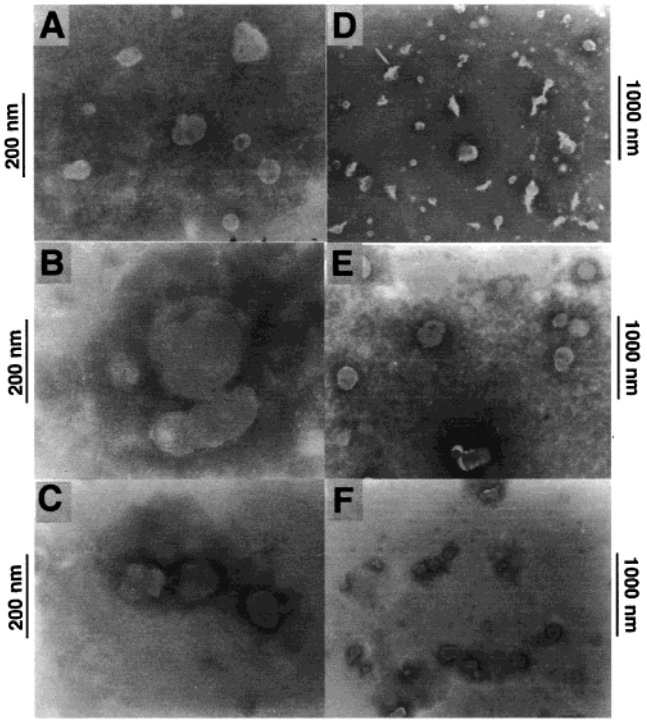

FIGURE 3: Peptide-induced lipid mixing as a result of membrane fusion. Electron micrographs of negatively stained PC LUV (A), LUV incubated for 10 min with MV-197 at a peptide/lipid molar ratio of 0.037 (B), and LUV incubated for 10 min with Mu-MV-197 at a peptide/lipid molar ratio of 0.037 (C) are shown. D−F correspond to A−C, respectively, with 5 times lower magnification.

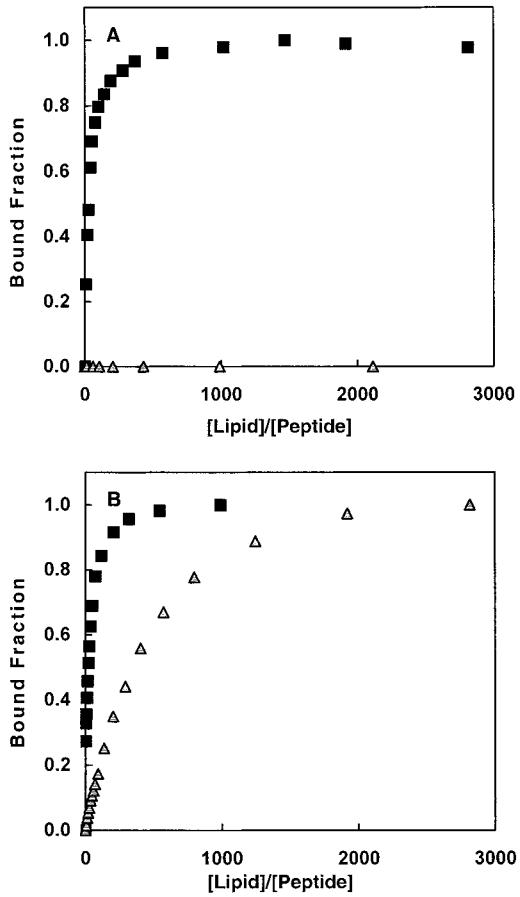

FIGURE 4: Membrane-binding affinities of MV-197 and Mu-MV-197. NBD-labeled peptides (0.1 μM) dissolved in PBS were titrated with PC (A) or PC/PG (1:1) (B) SUV. The fluorescence intensity was measured with the excitation wavelength set at 467 nm (8 nm slit) and the emission recorded at 530 nm (8 nm slit) and plotted as a function of the lipid/peptide molar ratio. Symbols: (■) MV-197; (gray triangle) Mu-MV-197.

the peptide binds PC/PG SUV at the lipid/peptide molar ratios used for the lipid-mixing assay. Although binding of the peptide to the membrane does not necessarily correlate with membrane fusion (*54*), it is a prerequisite. Thus, these results may account for the lack of detected fusion activity of Mu-MV-197 toward PC and PC/PG model membranes.

Insertion of MV-197 and Mu-MV-197 Amino Termini into a More Hydrophobic Environment upon Membrane Binding. Several fusion peptides were shown to have their N terminus inserted into the lipid bilayer (*18*, *26*, *41*). To determine the position of the N terminus of MV-197 with respect to the membrane, we monitored the fluorescence-emission spectra of NBD-labeled peptides before and after the addition of the vesicles. Specifically, the fluorescence-emission spectra of NBD-labeled MV-197 and Mu-MV-197 were measured in aqueous solution and in the presence of PC/PG (1:1) and, in the case of MV-197, also in the presence of PC SUV. The fluorescence-emission spectrum of Mu-MV-197 in PC SUV was not tested because, as is shown in Figure 4, no binding was detected. Both peptides displayed a shift toward lower wavelengths, with a concomitant increase in fluorescence-emission intensity after adding the vesicles (data not shown), indicating that the NBD-labeled peptides interact with the membrane. The maximal wavelengths of fluorescence emission were ∼527 nm for MV-197 with PC/PG or PC vesicles and ∼525 nm for Mu-MV-197 with PC/PG vesicles. A similar value has been obtained for the N-terminal fusion peptide of the Sendai virus (528 nm; *18*). Moreover, it has been shown that the maximum emission of NBD, inserted into the hydrophobic core of the membranes, is in the range of 526−529 nm, whereas higher values are obtained when the NBD is connected to the polar headgroup of phosphatidylethanolamine (535−537 nm; *48*). Thus, we conclude that, in their membrane-bound state, the N termini of both MV-197 and Mu-MV-197 are located in the hydrophobic core of the membrane.

Susceptibility of MV-197 and Mu-MV-197 to Proteolytic Digestion when Bound to Membranes. To further investigate the location of the peptides' backbones with respect to the plane of the membrane, we investigated the susceptibility of the membrane-bound peptides to proteolytic digestion. As previously shown, peptides located on the surface of the membrane are susceptible to proteolytic cleavage (*41*), whereas peptides located in the interior of the membrane are protected against cleavage (*55*). As shown in Figure 5A, adding Proteinase K to a mixture of NBD-labeled MV-197 and PC/PG (1:1) SUV resulted in a rapid decrease in the fluorescence of NBD, suggesting that the peptide was cleaved into small fragments that were released from the hydrophobic environment of the membrane. Similar results were obtained for NBD-labeled Mu-MV-197 (Figure 5C) and for a mixture of NBD-labeled MV-197 and PC SUV (data not shown). When the protease was added to the labeled peptides before adding the vesicles, a similar final level of NBD fluorescence intensity was observed (Figure 5, panels B and D). These results suggest that at least a part of the peptides' backbones is located on the surface of the membrane. Similar results

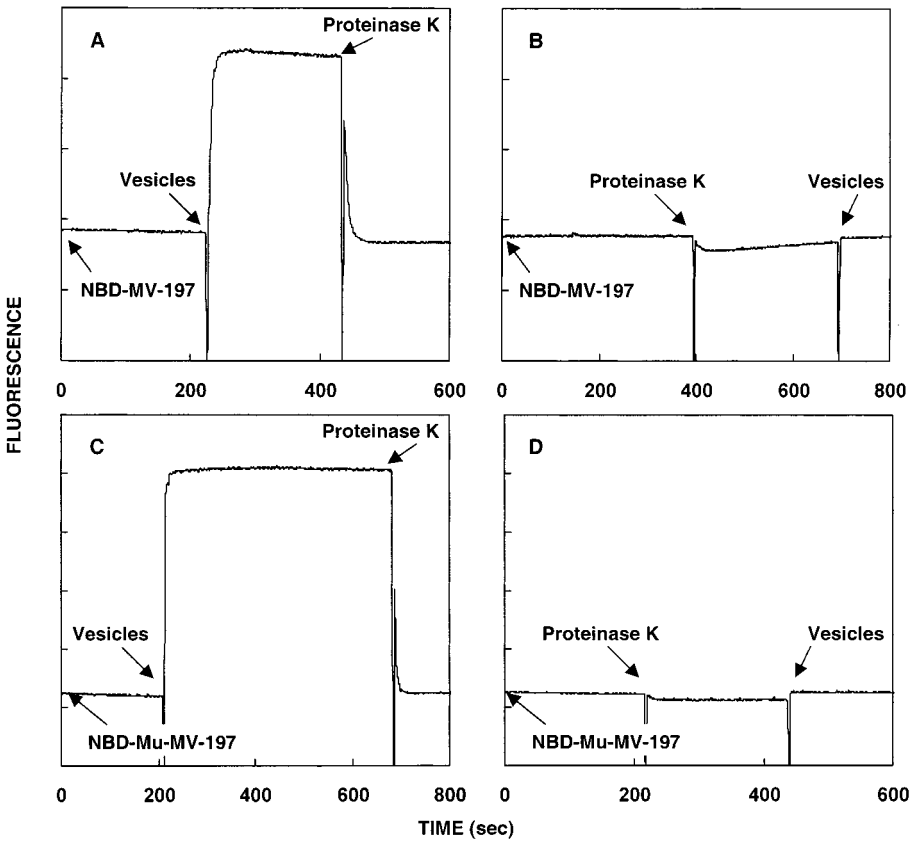

FIGURE 5: Susceptibility of MV-197 and Mu-MV-197 to enzymatic digestion when bound to membranes. The fluorescence emission of NBD-labeled peptides was monitored at 530 nm (8 nm slit), with the excitation set at 467 nm (8 nm slit). (A) PC/PG (1:1) SUV (100 μM) were added to 0.1 μM NBD-MV-197, followed by the addition of 20 μL of Proteinase K (10 mg/mL) (B) As a control experiment, 20 μL of Proteinase K (10 mg/mL) were added to 0.1 μM NBD-MV-197 before the addition of 100 μM PC/PG (1:1) SUV; (C and D) The same as indicated in A and B, respectively, but with NBD-Mu-MV-197 and 300 μM of PC/PG SUV.

have been obtained for the N-terminal fusion peptide of HIV-1 (*26*) and for the internal fusion peptide in the Sendai virus (*41*).

Oligomeric State of MV-197 and Mu-MV-197 in Solution and in the Membrane. Several known fusion peptides have been shown to form oligomers in their membrane-bound state (*18*, *26*, *41*). To determine the oligomeric states of the peptides in solution and in the membrane, we monitored the fluorescence intensities of the Rho-labeled peptides. The fluorescence intensity of Rhodamine is highly sensitive to homo energy transfer (self-quenching) but is only slightly affected by the dielectric constant of its surroundings. Therefore, changes in the fluorescence intensity of the Rho-labeled peptides may be attributed mainly to changes in their oligomeric states. In a typical experiment, Proteinase K was added to 1 μM Rho-labeled peptide, either in an aqueous solution or in the presence of PC/PG SUV. As depicted in Figure 6, the fluorescence intensity in an aqueous solution of Rho-labeled MV-197 significantly increased upon the addition of Proteinase K, suggesting that MV-197 forms oligomers in PBS. In contrast, no significant change in Rho-Mu-MV-197 fluorescence in solution was detected, implying no self-association of the scrambled peptide in solution. Nevertheless, when Proteinase K was added to membrane-bound Rho-MV-197 and Rho-Mu-MV-197, a decrease in Rhodamine fluorescence was observed. Similar results were obtained for Rho-MV-197 in PC SUV (data not shown). These results imply that the Rho-labeled peptides do not self-associate in their membrane-bound state. Moreover, the

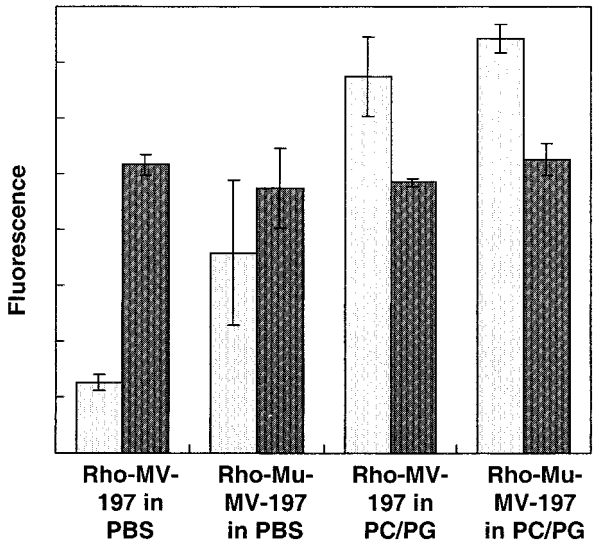

FIGURE 6: Oligomeric state of MV-197 and Mu-MV-197 in solution and in the membrane. Proteinase K (10 mg/mL) was added to 1 μM Rho-labeled peptides either in a PBS solution or in the presence of PC/PG (1:1) or PC SUV (3.2 or 8 mM). The fluorescence intensity at 578 nm (8 nm slit) was recorded as a function of time before and after the addition of the enzyme. The excitation was set at 530 nm (8 nm slit). Symbols: (light-gray bar) fluorescence intensity of the Rho-labeled peptides before the addition of Proteinase K; (dark bar) fluorescence intensity after the addition of Proteinase K.

decrease in fluorescence upon membrane detachment of the peptides derives from the slight influence of the membranous

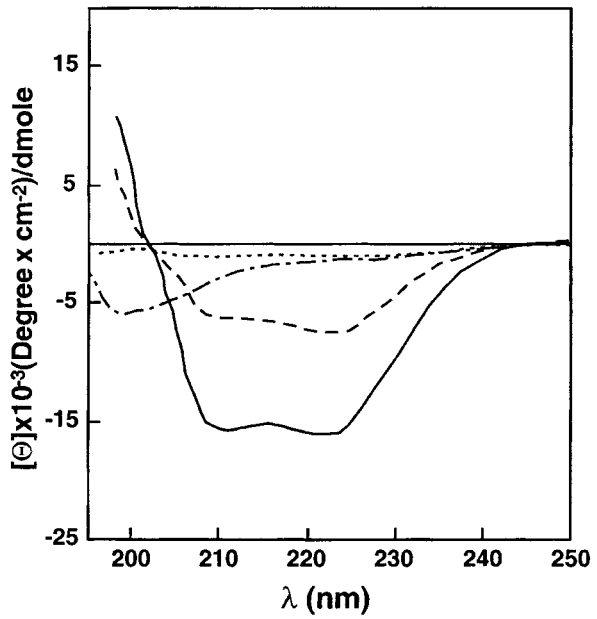

FIGURE 7: α-Helical content of MV-197 and Mu-MV-197 in membranes. Spectra were taken at peptide concentrations of 10 μM. Symbols: (···) MV-197 in PBS, (—) MV-197 in 5 mM PC/PG (1:1) SUV, (— · —) Mu-MV-197 in PBS, and (— —) Mu-MV-197 in 5 mM PC/PG (1:1) SUV.

environment on the Rhodamine fluorescence, as demonstrated by Mannuzzu et al. (*56*).

α*-Helical Content of MV-197 and Mu-MV-197 in Membranes*. The relevance of the membrane-binding ability was confirmed using CD. Whereas the spectrum of the peptides in PBS revealed no structure, they adopted an α-helical structure in the presence of membranes (Figure 7). The fractional helicities, calculated according to the elipticity at 222 nm (*51*) for MV-197 and Mu-MV-197 in PC/PG (1:1) SUV, are ∼45% and ∼17%, respectively, whereas for MV-197 in PC SUV the elipticity is ∼40% (data not shown). Note that the lipid/peptide molar ratio used to obtain the CD spectra of the peptides in the presence of vesicles was about 1:600. Experiments done with higher lipid/peptide ratios were not reliable because of light scattering. Under the conditions used, the approximate percentages of MV-197 and Mu-MV-197 that are bound to vesicles, as evaluated from their binding curves, are ∼98% and ∼68%, respectively (Figure 4). Nevertheless, even if the different levels of bound fractions of the peptides are taken into account, the difference in their CD spectra, in the presence of vesicles, is still apparent.

DISCUSSION

Two Fusion Peptides in the Paramyxoviridae F1 Protein. We showed here that a 29-residue peptide (MV-197) corresponding to amino acids 197−225 of the fusion protein of the measles virus (Figure 1C) is able to induce membrane fusion of LUV to a larger extent than the 33-amino acid N-terminal fusion peptide (Figure 2). MV-197 is located in the fusion protein of the measles virus in a region homologous to the internal fusion peptide recently found in the Sendai virus (*41*). Because the internal fusion peptide from the Sendai virus SV-201 has a homologous sequence to the N-terminal fusion peptide of HIV-1 (Figure 1B), its fusogenic ability can be attributed to its specific sequence. Thus, the existence of two fusion peptides in the Sendai virus fusion protein could have been a special case not related to the membrane-fusion mechanism of other paramyxoviruses. Hence, we decided to test whether there are two fusion peptides in the measles virus as well. We chose the measles virus because it belongs to the paramyxoviridae family, but its fusion protein has a low sequence homology compared to that of the fusion protein of the Sendai virus (*35*). The sequence of MV-197 is different from those of SV-201 and the N-terminal fusion peptide of HIV-1 in several major aspects (Figure 1B). Fusion peptides are thought to be relatively hydrophobic and rich in glycine (*4*). Accordingly, the alignment between SV-201 and HIV-1 N-terminal fusion peptide contains three conserved glycines (Figure 1B). On the other hand, two of these glycines are replaced in MV-197 by charged amino acids (one acidic and one basic). This was predicted to impair the ability of the peptide to cause membrane fusion because this kind of substitution in the N-terminal fusion peptide of SIV has been shown to abolish the fusogenic activity of the peptide (*9*). In addition, there is a proline in MV-197 instead of a serine present in the corresponding position in the Sendai and HIV-1 fusion peptides. The presence of a proline in this region could affect the structure of MV-197 compared to those of the other two fusion peptides and, thus, disturb its fusogenic activity. To conclude, although MV-197 was predicted not to be fusogenic on the basis of the major sequence differences from the internal fusion peptide of the Sendai F1 protein, it preserves the high fusogenic activity, as is expected for an internal fusion peptide. MV-197 is elongated by 13 amino acids in the N-terminal direction, beyond the region of homology between the Sendai and HIV-1 fusion proteins, which has been postulated to be important for fusogenic activity (*41*). Therefore, the results suggest that MV-197 can act as an internal fusion peptide in the context of the whole fusion protein of the measles virus. On the other hand, the scrambled peptide, which does not bind to PC SUV and binds with a low affinity to PC/PG (1:1) SUV (Figure 4), is not active in inducing membrane fusion of either type of liposomes. This suggests that the exact sequence and not the overall amino acid content accounts for this activity. Several internal fusion peptides contain a proline residue next to their center (*57*), which has been shown to be important for membrane fusion (*58*). Because the proline residues in MV-197 appear next to its C-terminal end, further studies should reveal whether a similar peptide, elongated in the C-terminal direction and containing the proline residue close to its center, is more active.

The N-terminal fusion peptide of the measles virus is homologous in sequence to N-terminal fusion peptides from other paramyxoviridae viruses (*35*). Therefore, it is generally accepted that this region of the fusion protein is directly responsible for the membrane-fusion process in the measles virus. However, to our knowledge, only indirect evidence was found, relating the formation of nonlamellar structures by this region with its fusogenic activity (*15*). Here, we found no fusogenic activity of the N-terminal fusion peptide of the measles virus toward PC/PG (1:1), PC, or PC/SM/Chol (9:9:2) LUV (Figure 2), in accordance with the low activity found for the N-terminal fusion peptide of the Sendai virus toward PC/PG (1:1) LUV (*41*). However, these results do not rule out a possible role for this segment in the actual

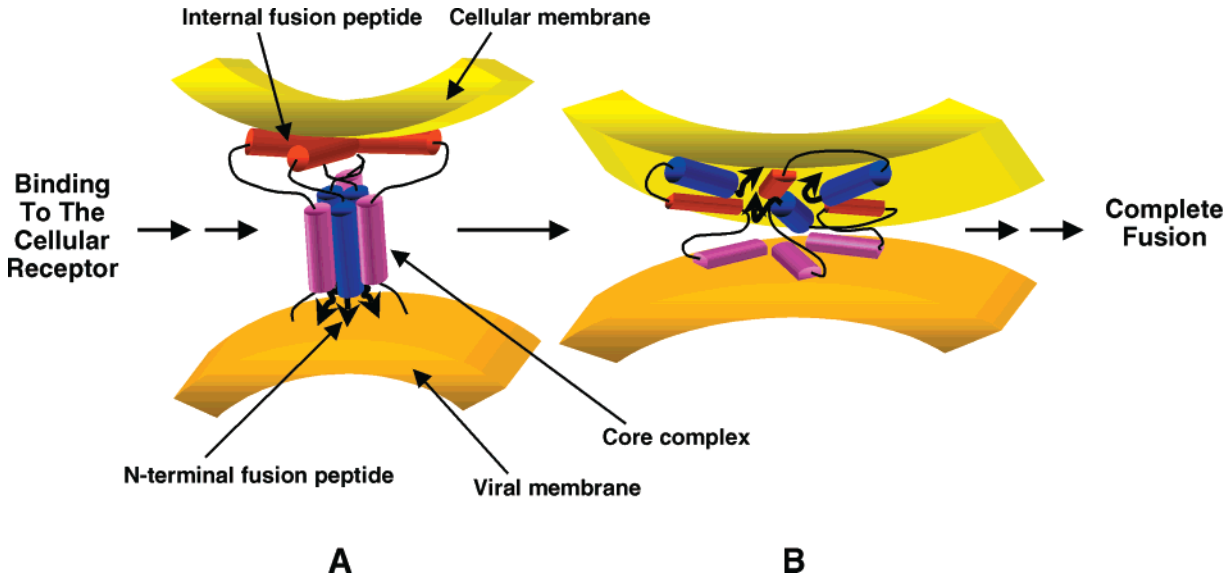

FIGURE 8: Model (adapted from Peisajovich et al. (*41*)) for paramyxoviridae-induced membrane fusion. Binding of the viral surface glycoprotein to the cellular receptor results in the formation of a trimeric core complex (blue and magenta) followed by the insertion of the internal fusion peptides (red) into the target membrane (A). Next, the core complex binds to the membranes and deoligomerizes therein (B). The N-terminal fusion peptide can then insert into the viral membrane and, together with the internal fusion peptide, facilitate the merging of the membranes.

membrane-fusion process, in the intact protein. Similarly, it has been shown that, although the fusion peptide of the Sendai virus has a low activity in inducing membrane fusion, a long peptide, composed of both the fusion peptide and the N-terminal heptad repeat of the Sendai F1 protein, has an increased activity (*28*).

The Internal Fusion Peptide is Highly Fusogenic in Biological Membrane Mimetic Environments. Many synthetic peptides corresponding to fusogenic regions of several viruses have been shown to induce fusion of liposomes (*14*, *16*−*19*, *26*, *28*, *29*). However, usually the liposomes were composed, at least in part, of negatively charged lipids or included PE, a factor known to facilitate membrane fusion (*59*, *60*). Nevertheless, MV-197 is highly active toward the more stable PC LUV, suggesting that the corresponding region in the full-length protein may act as a potent internal fusion peptide. In addition, the outer leaflet of human cellular membranes is composed mainly of PC, SM, and Chol, with a low portion of PE (*61*). Therefore, the testing of the peptide-induced fusion of PC/SM/Chol liposomes lacking PE is more relevant to the physiology of viral infection of human cells. Because the measles virus is a human pathogen (*2*), the activity of MV-197 toward PC/SM/Chol LUV may suggest a similar activity of the corresponding region of the protein toward the target cells' membranes.

Structural Characterization and Organization in the Membrane of the Internal Fusion Peptide. Oblique orientation with respect to the plane of the membrane was found for several viral fusion peptides, including influenza (*62*), HIV-1 (*27*), SIV (*16*), the Sendai virus (*18*), the bovine leukemia virus (*63*), the Newcastle disease virus (*64*), and the measles virus (*65*). It has been suggested that peptides inserted into membranes at an oblique angle may disturb the packing of the membrane by expanding the interior of the membrane relative to its surface (*66*). This is expected to increase negative curvature strain and support the formation of inverted phases, which may promote membrane fusion. Here, we studied the extent of the penetration of MV-197 and its scrambled mutant into lipid bilayers, analyzing the change in the fluorescence of NBD-labeled peptides upon the addition of vesicles. We found that the N termini of both peptides are inserted into the hydrophobic core of the membranes. Nevertheless, the peptides were susceptible to enzymatic digestion in their membrane-bound state (Figure 5), suggesting that at least part of their backbone is exposed to the surface of the membrane. The kinetics of digestion might depend on the binding equilibrium of the peptide to the membrane. However, the kinetics of digestion observed in this study (Figure 5) are very fast, implying that at least part of the peptides' backbone is exposed to the surface of the membrane and, thus, digested fast and released from the membrane. If the peptides were inserted deep into the membrane, we would have expected that the kinetics of their digestion would be dependent on the equilibrium with their soluble form. Moreover, as revealed with δ-endotoxin-α5 (*55*), with a leucine zipper in the cytoplasmic tail of HIV-1 gp-41 (*67*), and with the human antimicrobial peptide LL-37 (*68*), these peptides were practically not digested at all under similar conditions. The results obtained may suggest that the two peptides adopt an oblique orientation with respect to the surface of the membrane, although the possibility that the peptides are partially inserted in a direction perpendicular to the surface of the membrane cannot be ruled out. Nevertheless, FTIR experiments confirm that these peptides adopt an oblique orientation in a lipidic environment (unpublished data).

An α-helical structure seems to be important for promoting the activity of fusion peptides (*69*, *70*). Accordingly, we found that the fusogenic MV-197, although containing two prolines, has a high α-helical content in its membrane-bound state (Figure 7). These results are in agreement with the finding that the helical propensity of proline is greatly enhanced in the environment of the membrane (*71*). Furthermore, the inactive scrambled mutant Mu-MV-197 has a lower helical content, even when taking into account that only about 68% of the peptides were bound to membranes

in the lipid/peptide molar ratio used.

Fusion proteins are believed to be oligomers in their active conformation (*22*, *72*). Furthermore, there is evidence suggesting that the oligomeric state of membrane-bound fusion peptides is important for their activity (*26*). Here, we utilized the change in fluorescence of the Rho-labeled peptides to test whether MV-197 and its scrambled mutant self-associate in solution and in lipid vesicles. Importantly, we found that MV-197, although highly fusogenic and oligomeric in solution, does not self-associate in its membrane-bound state, whereas its inactive mutant is a monomer in solution and in the membrane (Figure 6). These results are in accordance with what was reported by Pecheur and co-workers, who found that for a membrane-anchored peptide oligomerization is not an absolute prerequisite for inducing membrane fusion (*73*). Moreover, Macosko et al. demonstrated that although the HA2 protein of the influenza virus is trimeric its fusion peptide is likely to be a monomer in the membrane (*74*). The kinetics of membrane fusion induced by MV-197 is very fast (see insets of Figure 2), and the peptide approaches the membrane from solution as an oligomer with unknown dissociation kinetics. Therefore, we cannot rule out the possibility that during the fusion process the peptide is still self-associated and slowly dissociates only afterward. The inactive scrambled mutant may be, in this case, inactive because of the lack of self-association in solution. This issue can be a subject for further investigation and may lead to a better understanding of the actual process.

Synthetic peptides, corresponding to segments of proteins, are widely used for investigating protein−membrane interactions in general (*55*, *75*−*79*) and viral-induced membrane fusion in particular (*14*−*19*). The motivation for using this approach is that it allows us to address questions regarding specific interactions between regions of proteins and membranes. Nevertheless, it is important to confirm that the synthetic peptide appropriately represents its corresponding segment in the full-length protein (*80*, *81*). In the case of the measles virus internal fusion peptide, several properties that were demonstrated in this study, such as binding to membranes and the ability to fuse them, orientation in the membrane-bound state, and α-helical secondary structure, were proposed to be features of viral protein-induced membrane fusion (*4*).

In conclusion, the results of this study suggest that the existence of two fusion peptides, one located at the N terminus and one located at the interior of the F1 protein, is a common feature of paramyxoviruses. This study supports our recently revised model for membrane fusion induced by the paramyxovirus F protein (*41*). As shown in Figure 8, the model, adapted from Peisajovich et al. (*41*), suggests that binding of the viral surface glycoprotein to cell receptors results in a refolding of the F protein into a trimeric coiled coil (core complex). This conformation has previously been observed by X-ray crystallography for the homologous SV5 F protein (*82*). The process may continue by insertion of the internal fusion peptides into the target membrane (Figure 8A). However, we cannot rule out the possibility that the N-terminal fusion peptide binds to the target membrane first. Then, the binding of the core complex to the membrane causes an "umbrella"-like opening of the complex (*40*; Figure 8B). This membrane-induced conformational change enables the approach of the viral and cellular membranes. The final merging of the two membranes is induced by both the N-terminal and the internal fusion peptides.

ACKNOWLEDGMENT

We thank Dr. Y. Marikovsky for his help in visualization of the phospholipid vesicles using electron microscopy and S. G. Peisajovich for his technical assistance and fruitful discussion.

REFERENCES

1. Lamb, R. A., and Kolakofsky, D. (1996) in *Virology* (Fields, B. N., Knipe, D. M., and Howley, P. M., Eds.), pp 1177−1204, Lippincott-Raven, Philadelphia, PA.
2. Griffin, D. E., and Bellini, W. J. (1996) in *Virology* (Fields, B. N., Knipe, D. M., and Howley, P. M., Eds.), pp 1267−1312, Lippincott-Raven, Philadelphia, PA.
3. Stegmann, T., Doms, R. W., and Helenius, A. (1989) *Annu. Rev. Biophys. Biophys. Chem. 18*, 187−211.
4. White, J. M. (1990) *Annu. Rev. Physiol. 52*, 75−97.
5. White, J., Kielian, M., and Helenius, A. (1983) *Q. Rev. Biophys. 16*, 151−195.
6. Blumberg, B. M., Giorgi, C., Rose, K., and Kolakofsky, D. (1985) *J. Gen. Virol. 66*, 317−331.
7. Gething, M. J., Doms, R. W., York, D., and White, J. (1986) *J. Cell Biol. 102*, 11−23.
8. Gallaher, W. R. (1987) *Cell 50*, 327−328.
9. Bosch, M. L., Earl, P. L., Fargnoli, K., Picciafuoco, S., Giombini, F., Wong-Staal, F., and Franchini, G. (1989) *Science 244*, 694−697.
10. Hunter, E., Hill, E., Hardwick, M., Bhown, A., Schwartz, D. E., and Tizard, R. (1983) *J. Virol. 46*, 920−936.
11. Whitt, M. A., Zagouras, P., Crise, B., and Rose, J. K. (1990) *J. Virol. 64*, 4907−4913.
12. Gallaher, W. R. (1996) *Cell 85*, 477−478.
13. Luo, Z., and Weiss, S. R. (1998) *Virology 244*, 483−494.
14. Rafalski, M., Lear, J. D., and DeGrado, W. F. (1990) *Biochemistry 29*, 7917−7922.
15. Yeagle, P. L., Epand, R. M., Richardson, C. D., and Flanagan, T. D. (1991) *Biochim. Biophys. Acta 1065*, 49−53.
16. Martin, I., Dubois, M. C., Defrise-Quertain, F., Saermark, T., Burny, A., Brasseur, R., and Ruysschaert, J. M. (1994) *J. Virol. 68*, 1139−1148.
17. Nieva, J. L., Nir, S., Muga, A., Goni, F. M., and Wilschut, J. (1994) *Biochemistry 33*, 3201−3209.
18. Rapaport, D., and Shai, Y. (1994) *J. Biol. Chem. 269*, 15124−15131.
19. Ruiz-Arguello, M. B., Goni, F. M., Pereira, F. B., and Nieva, J. L. (1998) *J. Virol. 72*, 1775−1781.
20. Duzgunes, N., and Gambale, F. (1988) *FEBS Lett. 227*, 110−114.
21. Burger, K. N., Wharton, S. A., Demel, R. A., and Verkleij, A. J. (1991) *Biochim. Biophys. Acta 1065*, 121−129.
22. Freed, E. O., Delwart, E. L., Buchschacher, G. L., Jr., and Panganiban, A. T. (1992) *Proc. Natl. Acad. Sci. U.S.A 89*, 70−74.
23. Horvath, C. M., and Lamb, R. A. (1992) *J. Virol. 66*, 2443−2455.
24. Pereira, F. B., Goni, F. M., and Nieva, J. L. (1995) *FEBS Lett. 362*, 243−246.
25. Martin, I., Schaal, H., Scheid, A., and Ruysschaert, J. M. (1996) *J. Virol. 70*, 298−304.
26. Kliger, Y., Aharoni, A., Rapaport, D., Jones, P., Blumenthal, R., and Shai, Y. (1997) *J. Biol. Chem. 272*, 13496−13505.
27. Pritsker, M., Rucker, J., Hoffman, T. L., Doms, R. W., and Shai, Y. (1999) *Biochemistry 38*, 11359−11371.
28. Ghosh, J. K., and Shai, Y. (1999) *J. Mol. Biol. 292*, 531−546.
29. Wharton, S. A., Martin, S. R., Ruigrok, R. W., Skehel, J. J., and Wiley, D. C. (1988) *J. Gen. Virol. 69*, 1847−1857.
30. Pereira, F. B., Goni, F. M., and Nieva, J. L. (1997) *AIDS Res. Hum. Retroviruses 13*, 1203−1211.
31. Homma, M., and Ohuchi, M. (1973) *J. Virol. 12*, 1457−1465.

32. Scheid, A., and Choppin, P. W. (1977) *Virology 80*, 54−60.
33. Hardwick, J. M., and Bussell, R. H. (1978) *J. Virol. 25*, 687−692.
34. Gething, M. J., White, J. M., and Waterfield, M. D. (1978) *Proc. Natl. Acad. Sci. U.S.A. 75*, 2737−2740.
35. Richardson, C., Hull, D., Greer, P., Hasel, K., Berkovich, A., Englund, G., Bellini, W., Rima, B., and Lazzarini, R. (1986) *Virology 155*, 508−523.
36. Yu, Y. G., King, D. S., and Shin, Y. K. (1994) *Science 266*, 274−276.
37. Epand, R. F., Macosko, J. C., Russell, C. J., Shin, Y. K., and Epand, R. M. (1999) *J. Mol. Biol. 286*, 489−503.
38. Rabenstein, M., and Shin, Y. K. (1995) *Biochemistry 34*, 13390−13397.
39. Ghosh, J. K., and Shai, Y. (1998) *J. Biol. Chem. 273*, 7252−7259.
40. Ben-Efraim, I., Kliger, Y., Hermesh, C., and Shai, Y. (1999) *J. Mol. Biol. 285*, 609−625.
41. Peisajovich, S. G., Samuel, O., and Shai, Y. (2000) *J. Mol. Biol. 296*, 1353−1365.
42. Merrifield, R. B., Vizioli, L. D., and Boman, H. G. (1982) *Biochemistry 21*, 5020−5031.
43. Shai, Y., Bach, D., and Yanovsky, A. (1990) *J. Biol. Chem. 265*, 20202−20209.
44. Rapaport, D., and Shai, Y. (1992) *J. Biol. Chem. 267*, 6502−6509.
45. Shai, Y., Hadari, Y. R., and Finkels, A. (1991) *J. Biol. Chem. 266*, 22346−22354.
46. Struck, D. K., Hoekstra, D., and Pagano, R. E. (1981) *Biochemistry 20*, 4093−4099.
47. Tiller, G. E., Mueller, T. J., Dockter, M. E., and Struve, W. G. (1984) *Anal. Biochem. 141*, 262−266.
48. Rajarathnam, K., Hochman, J., Schindler, M., and Ferguson-Miller, S. (1989) *Biochemistry 28*, 3168−3176.
49. Schwarz, G., Stankowski, S., and Rizzo, V. (1986) *Biochim. Biophys. Acta 861*, 141−151.
50. Rapaport, D., Ovadia, M., and Shai, Y. (1995) *EMBO J. 14*, 5524−5531.
51. Wu, C. S. C., Ikeda, K., and Yang, J. T. (1981) *Biochemistry 20*, 566−570.
52. Rapaport, D., and Shai, Y. (1991) *J. Biol. Chem. 266*, 23769−23775.
53. Gazit, E., Boman, A., Boman, H. G., and Shai, Y. (1995) *Biochemistry 34*, 11479−11488.
54. Ghosh, J. K., Peisajovich, S. G., and Shai, Y. (2000) *Biochemistry 39*, 11581−11592.
55. Gazit, E., and Shai, Y. (1993) *Biochemistry 32*, 3429−3436.
56. Mannuzzu, L. M., Moronne, M. M., and Isacoff, E. Y. (1996) *Science 271*, 213-216.
57. White, J. M. (1992) *Science 258*, 917−924.
58. Delos, S. E., Gilbert, J. M., and White, J. M. (2000) *J. Virol. 74*, 1686−1693.
59. Martin, I., Defrise-Quertain, F., Decroly, E., Vandenbranden, M., Brasseur, R., and Ruysschaert, J. M. (1993) *Biochim. Biophys. Acta 1145*, 124−133.
60. Chernomordik, L., Kozlov, M. M., and Zimmerberg, J. (1995) *J. Membr. Biol. 146*, 1−14.
61. Vance, D. E., and Vance, J. (1991) in *New Comprehensive Biochemistry* (Neuberger, A., and Van Deenen, L. L. M., Eds.), pp 1−41, Elsevier Science Publishers B. V., Amsterdam, The Netherlands.
62. Tatulian, S. A., Hinterdorfer, P., Baber, G., and Tamm, L. K. (1995) *EMBO J. 14*, 5514−5523.
63. Voneche, V., Portetelle, D., Kettmann, R., Willems, L., Limbach, K., Paoletti, E., Ruysschaert, J. M., Burny, A., and Brasseur, R. (1992) *Proc. Natl. Acad. Sci. U.S.A. 89*, 3810−3814.
64. Brasseur, R. (1991) *J. Biol. Chem. 266*, 16120−16127.
65. Brasseur, R., Vandenbranden, M., Cornet, B., Burny, A., and Ruysschaert, J. M. (1990) *Biochim. Biophys. Acta 1029*, 267−273.
66. Epand, R. F., Martin, I., Ruysschaert, J. M., and Epand, R. M. (1994) *Biochem. Biophys. Res. Commun. 205*, 1938−1943.
67. Kliger, Y., and Shai, Y. (1997) *Biochemistry 36*, 5157−5169.
68. Oren, Z., Lerman, J. C., Gudmundsson, G. H., Agerberth, B., and Shai, Y. (1999) *Biochem. J. 341*, 501−513.
69. Lee, S., Aoki, R., Oishi, O., Aoyagi, H., and Yamasaki, N. (1992) *Biochim. Biophys. Acta 1103*, 157−162.
70. Rapaport, D., Hague, G. R., Pouny, Y., and Shai, Y. (1993) *Biochemistry 32*, 3291−3297.
71. Li, S. C., Goto, N. K., Williams, K. A., and Deber, C. M. (1996) *Proc. Natl. Acad. Sci. U.S.A. 93*, 6676−6681.
72. Wahlberg, J. M., Bron, R., Wilschut, J., and Garoff, H. (1992) *J. Virol. 66*, 7309−7318.
73. Pecheur, E. I., Sainte-Marie, J., Bienvenue, A., and Hoekstra, D. (1999) *Biochemistry 38*, 364−373.
74. Macosko, J. C., Kim, C. H., and Shin, Y. K. (1997) *J. Mol. Biol. 267*, 1139−1148.
75. Buck, C. A., and Horwitz, A. F. (1987) *J. Cell Sci. Suppl. 8*, 231−250.
76. Lentz, T. L., Hawrot, E., Donnelly-Roberts, D., and Wilson, P. T. (1988) *Adv. Biochem. Psychopharmacol. 44*, 57−71.
77. Jones, J. D., McKnight, C. J., and Gierasch, L. M. (1990) *J. Bioenerg. Biomembr. 22*, 213−232.
78. Peled, H., and Shai, Y. (1993) *Biochemistry 32*, 7879−7885.
79. Thellung, S., Florio, T., Corsaro, A., Arena, S., Merlino, M., Salmona, M., Tagliavini, F., Bugiani, O., Forloni, G., and Schettini, G. (2000) *Int. J. Dev. Neurosci. 18*, 481−492.
80. Epand, R. M., Cheetham, J. J., Epand, R. F., Yeagle, P. L., Richardson, C. D., Rockwell, A., and Degrado, W. F. (1992) *Biopolymers 32*, 309−314.
81. Duzgunes, N., and Shavnin, S. A. (1992) *J. Membr. Biol. 128*, 71−80.
82. Baker, K. A., Dutch, R. E., Lamb, R. A., and Jardetzky, T. S. (1999) *Mol. Cell 3*, 309−319.

BI001533N